Bioorganic & Medicinal Chemistry Letters 19 (2009) 6507–6514

Contents lists available at ScienceDirect

Bioorganic & Medicinal Chemistry Letters

journal homepage: www.elsevier.com/locate/bmcl

Discovery and optimization of antibacterial AccC inhibitors

Cliff C. Cheng [a,*], Gerald W. Shipps Jr. [a], Zhiwei Yang [a,†], Binyuan Sun [a], Noriyuki Kawahata [a,‡], Kyle A. Soucy [a], Aileen Soriano [b], Peter Orth [b], Li Xiao [b], Paul Mann [b], Todd Black [b]

[a] Schering-Plough Research Institute, 320 Bent Street, Cambridge, MA 02141, United States
[b] Schering-Plough Research Institute, 2015 Galloping Hill Road, Kenilworth, NJ 07033, United States

ARTICLE INFO

Article history:
Received 20 August 2009
Revised 12 October 2009
Accepted 13 October 2009

Keywords:
Biotin carboxylase
AccC
Acetyl coenzyme-A carboxylase
ACCase
BCCP
Biotin carboxyl carrier protein
Structure Based Drug Design (SBDD)
ALIS: Automated Ligand Identification System
AS-MS: Affinity-Selection Mass Spectrometry
HS294 E. coli
MIC

ABSTRACT

The biotin carboxylase (AccC) is part of the multi-component bacterial acetyl coenzyme-A carboxylase (ACCase) and is essential for pathogen survival. We describe herein the affinity optimization of an initial hit to give 2-(2-chlorobenzylamino)-1-(cyclohexylmethyl)-1*H*-benzo[*d*]imidazole-5-carboxamide (**1**), which was identified using our proprietary Automated Ligand Identification System (ALIS).[1] The X-ray co-crystal structure of **1** was solved and revealed several key interactions and opportunities for further optimization in the ATP site of AccC. Structure Based Drug Design (SBDD) and parallel synthetic approaches resulted in a novel series of AccC inhibitors, exemplified by (*R*)-2-(2-chlorobenzylamino)-1-(2,3-dihydro-1*H*-inden-1-yl)-1*H*-imidazo[4,5-*b*]pyridine-5-carboxamide (**40**). This compound is a potent and selective inhibitor of bacterial AccC with an IC_{50} of 20 nM and a MIC of 0.8 μg/mL against a sensitized strain of *Escherichia coli* (HS294 *E. coli*).

The emergence of antibiotic resistance continues to be a major health problem.[2] The development of broad spectrum antibiotics directed against novel targets is an important strategy to meet the urgent need for new antimicrobial agents. In this regard, the enzyme components of bacterial acetyl coenzyme-A carboxylase (ACCase) are excellent targets for antimicrobial drug discovery.[3] ACCase catalyzes the first committed step in fatty acid biosynthesis and is essential for bacterial viability.[4,5] It is a multi-component system comprised of two enzymes (AccC and AccAD) and the biotin carrier protein (BCCP or AccB).[6] The ACCase-catalyzed reaction can be divided into two half-reactions (Fig. 1). The first half-reaction, the ATP-dependent carboxylation of biotin, is catalyzed by AccC (biotin carboxylase) and uses bicarbonate as the carbon dioxide source. In the second half-reaction, catalyzed by AccA/D (carboxyltransferase), the carboxy group is transferred from biotin to acetyl-CoA to form the final product, malonyl-CoA. The biotin cofactor is attached to a lysine residue on BCCP and cycles between the two half-reactions.

At the amino acid level the ACCase components are highly conserved across all bacterial genera making ACCase an ideal broad spectrum target. The pyrrolidine dione antibiotics, for example, have broad spectrum antibacterial activity due to inhibition of AccA/D.[7] Although ACCase activity is also found in eukaryotic cells, the three functionalities required for catalysis are located in a single protein (Type I ACCase) which is distinct from the individual proteins employed by bacteria (Type II ACCase). These differences in active site organization suggest the potential to find specific inhibitors of the bacterial ACCase.

Using a proprietary AS-MS platform (the Automated ligand Identification System, ALIS) to screen a soluble version of the AccC protein we identified a series of benzimidazoles as AccC ligands from a mixture-based combinatorial library[8] and these preliminary hits were subsequently confirmed as low micromolar enzyme inhibitors.[11] Here, we describe the rapid hit-to-lead optimization of this series using mixture-based optimization and computer-aided drug design.

One of the initial hits, 2-(2-chlorobenzylamino)-1-(cyclohexylmethyl)-1*H*-benzo[*d*]imidazole-5-carboxamide (**1**) (Fig. 2)

* Corresponding author.
E-mail address: ccheng@alum.mit.edu (C.C. Cheng).
† Present address: Life Technologies, 5791 Van Allen Way, Carlsbad, CA 92008, United States.
‡ Present address: Aileron Therapeutics, Inc., 840 Memorial Dr., Cambridge, MA 02139, United States.

0960-894X/$ - see front matter © 2009 Elsevier Ltd. All rights reserved.
doi:10.1016/j.bmcl.2009.10.057

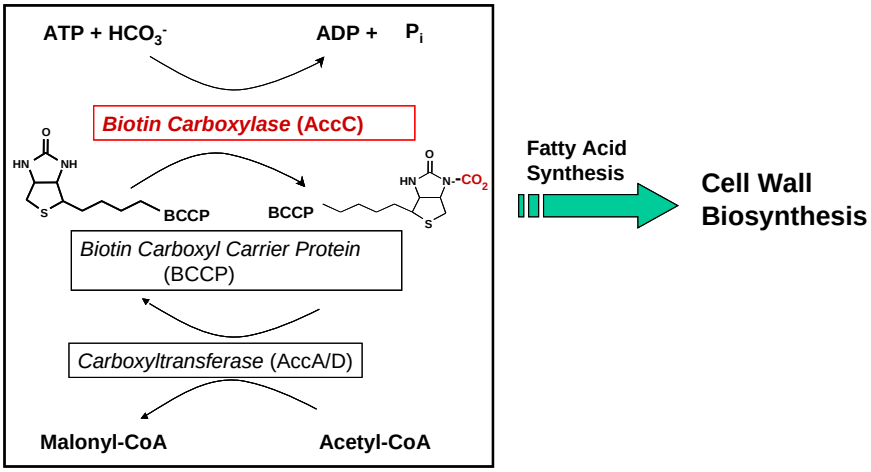

Figure 1. The conversion of acetyl-CoA to malonyl-CoA takes place in two steps. Biotin carboxylase catalyzes the first reaction by transferring CO_2 in an ATP-dependent fashion from bicarbonate to the biotin moiety of BCCP (or AccB), resulting in carboxybiotinoyl-BCCP. The CO_2 group is subsequently transferred from the carboxybiotin moiety to acetyl-CoA by the carboxyltransferase subunits, resulting in malonyl-CoA formation.

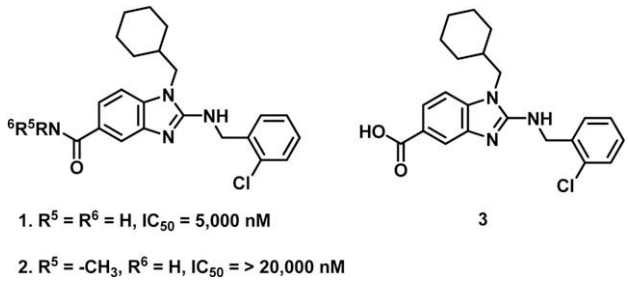

Figure 2. Initial benzimidazole carboxamide-based AccC ATP-site inhibitors.

was amendable to X-ray co-crystallography and its structure with the AccC protein was rapidly solved. Figure 3 illustrates the key compound–protein interactions.

Several hydrogen bonding interactions with AccC protein residues were noticed, particularly the primary amide of **1** H-bonded with Glu201 and Lys202 and this observation explained some of the preliminary negative SAR. For example, the methylated compound **2** (Fig. 2) was significantly less potent than initial hit and the carboxylic acid analog **3** (Fig. 2) was not detected during ALIS screening nor did it show activity in the biochemical assay. The NH of *o*-chlorobenzylamine was within H-bond distance from Glu288 and the polarized *o*-Cl was well positioned towards Tyr199. It was also observed that the *o*-chlorophenyl of the eastern region fit well inside the protein hydrophobic pocket. However, initial X-ray crystallography revealed that there might be nonproductive interactions between the cyclohexyl group and the protein surface at the northern region; additionally, two polar residues, His209 and Glu276, are located in this region. Based on the X-ray crystal structure of **1**, we initiated a hit optimization effort using structure-based drug design (SBDD).

The X-ray crystal structure and the initial SAR suggested that the interactions of the primary amide with protein residues were critical; focusing our chemistry efforts on the northern part of the molecule to incorporate hydrophobic and polar substituents. To access the northern part of the molecule quickly and efficiently, our strategy was to leverage the established chemistry from the parent combinatorial library to create focused, SAR informing sub-libraries[9] and then screen these sets using the ALIS platform.[1] Guided by the X-ray derived structural information approximately 300 mass-encoded, mixture-based compounds were synthesized on solid-phase using split/pool techniques. The syntheses of the mixture libraries are outlined in Scheme 1. 4-Fluoro-3-nitrobenzoic

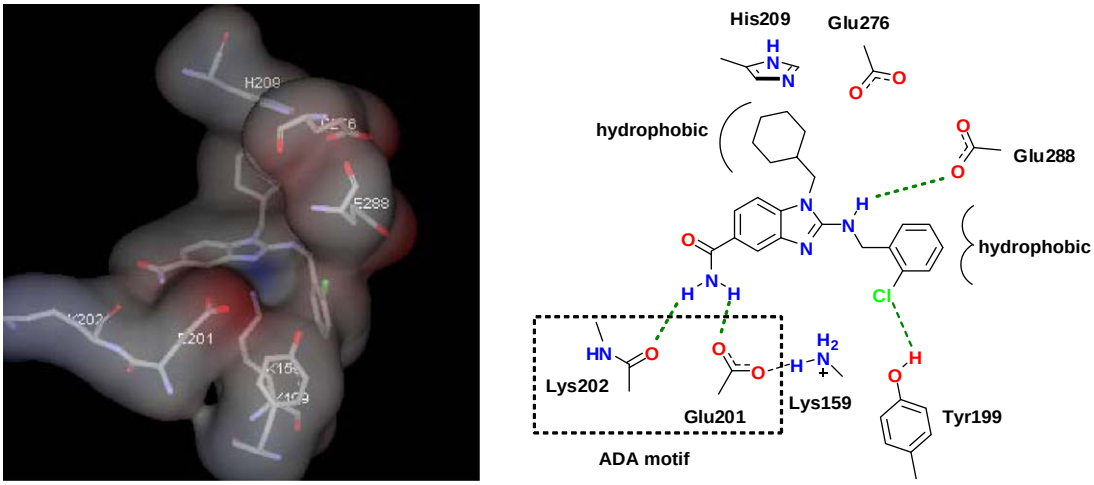

Figure 3. X-ray crystal structure of **1** bound to AccC ATP-site. PDB code 3JZF.

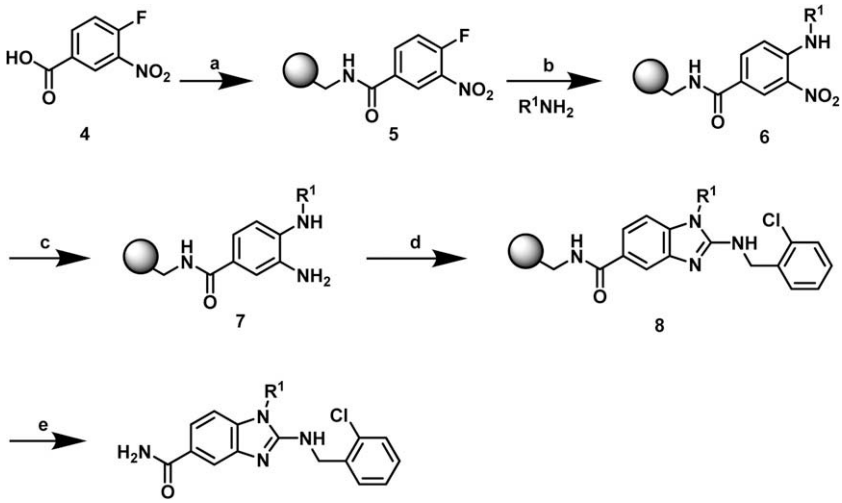

Scheme 1. Optimization of the northern part of the series using solid-phase synthesis. Reagents and condition: (a) $(COCl)_2$, DMF (cat.) then Rink resin, DCM, DIEA, 4 °C; (b) R^1NH_2, DIEA; (c) $SnCl_2$; (d) DIC, 2-chlorobenzyl isothiocyanate; (e) TFA, H_2O.

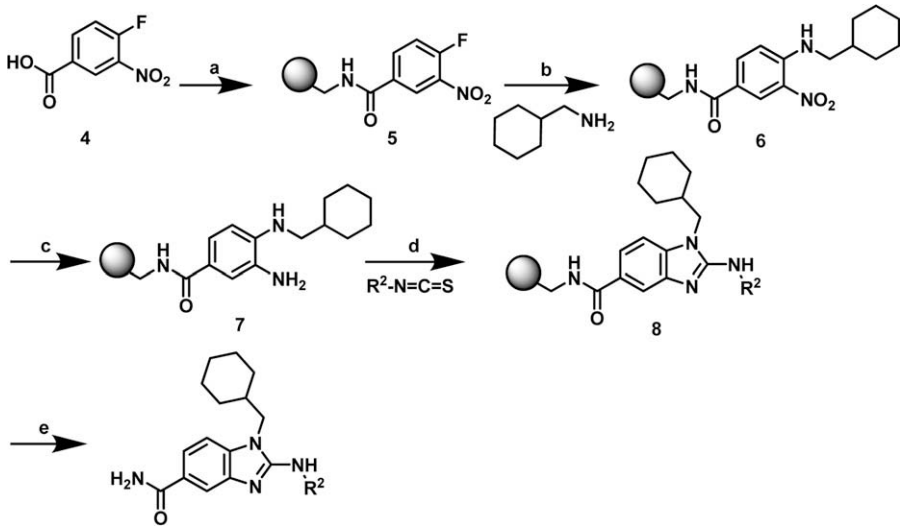

Scheme 2. Synthesis of the eastern analogs. Reagents and condition: (a) $(COCl)_2$, DMF (cat.) then Rink resin, DCM, DIEA, 4 °C; (b) cyclohexylmethanamine, DIEA; (c) $SnCl_2$; (d) DIC, R^2NCS; (e) TFA, H_2O.

acid was converted into acid chloride followed by amide formation with Rink resin. Amine building blocks (R^1NH_2) were reacted in the subsequent SNAr reaction to install the diversification point. The nitro group was reduced to the amine (**7**) by $SnCl_2$ and then reacted with 2-chlorobenzyl isothiocyanate to give the benzimidazoles. The mixture-based combinatorial libraries were cleaved from the resin by TFA, and the reaction outcomes verified by LC–MS, revealing that a minimum 85% of desired products were observed in amounts sufficient for potential detection as ligands to AccC.

ALIS screening revealed 16 compounds to be of potential interest and these compounds were synthesized separately, purified to >90% by preparative LC–MS and confirmed in the enzyme inhibition assay. The results are summarized in Table 1.

Informed by compound **1** and the new ligands we continued the optimization process by investigating the northern part (R^1) of benzimidazole (Table 1). From the early X-ray crystal structure of **1** it was observed that the cyclohexyl occupied the hydrophobic pocket. Compounds (**9** to **14**) with larger hydrophobic R^1 have shown better hydrophobic interactions and the aromatic group of compounds (**9** to **14**) might make additional interactions with the side chain of adjacent His209. It was suggested that the protein residues might be flexible at this region. Introducing H-bond donor hydroxyl group in compounds (**15** to **18**) provided good improvement in potency due to the polar interactions with protein residues of the northern binding pocket. Moreover, the second X-ray crystal structure of compound (**16**) was also resolved (data not shown) and provided clearer optimization guidance.

We further explored the possible opportunity to improve potency by designing compounds to enhance the interaction with Glu288 and Tyr199 residues at the eastern region. The facile, parallel synthesis chemistry is outlined in Scheme 2 and the results summarized in Table 2.

Modifications of the eastern part of the molecules resulted in significant loss of activity as we observed in the crystal structure. It was concluded that *o*-chlorobenzyl group is an optimal component

Table 1
Optimization of the northern part of benzimidazole

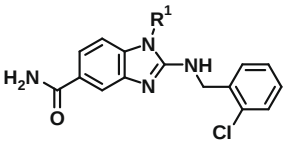

Compound	Structure of R^1	ACCase, IC_{50}[a,b] (μM)
1	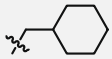	5
9	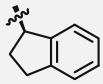	0.7
10	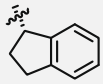	14.7
11	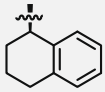	1.3
12	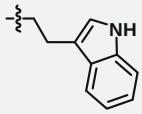	9.5
13	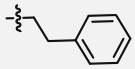	8.9
14		2.1
15	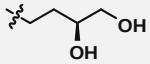	0.4
16	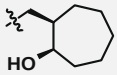	0.5
17		0.7
18	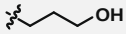	2

[a] Values are means of duplicate experiments on two separate weightings.
[b] [ATP] = 100 μM.

Table 2
Eastern part of benzimidazole modifications

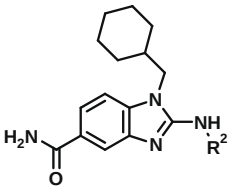

Compound	Structure of R^2	ACCase, IC_{50}[a,b] (μM)
19	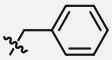	15.8
20	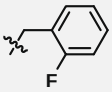	16.9
21	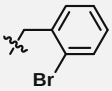	143
22	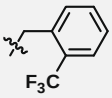	144
23	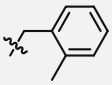	28
24	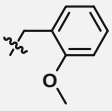	139
25	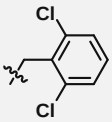	241
26	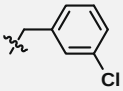	40
27	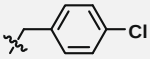	63
28	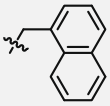	171
29	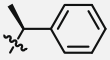	41

[a] Values are means of duplicate experiments on two separate weightings.
[b] [ATP] = 100 μM.

of this series to fit into the eastern pocket. Therefore, it is not surprising that analogs (**19** to **29**) are less active than compound (**1**) (Table 2).

Computer modeling results suggested the 4-position C–H of benzimidazole carboxamide could be replaced with a nitrogen atom (Fig. 4). The repulsive interaction of C–H at that position would be turned into an H-bond to interact with charged Lys159. Therefore compound (**35**) was considered to validate this idea and the synthesis is outlined in Scheme 3. We started from intermediate (**30**) which was subsequently methylated with TMS-diazomethane to give phenol ether (**31**). Oxidation of **31** with selenium dioxide gave a carboxylic acid followed by methylation to afford methyl ester (**32**). The SNAr reaction to displace the methoxy group of **32** with a primary amine (Table 3) followed by reduction gave compound (**34**), which was treated with isothiocyanates to give the cyclized aza-benzimidazole. The methyl ester was converted into a primary amide by aminolysis to give compound (**35**). As suggested by computer modeling, compounds (**36**), (**48**) and (**49**) with a N at the 4-position gained 10–20-fold in biochemical activity compared to compounds (**9**), (**17**) and (**18**). The results are listed in Table 3.

From X-ray crystallography and modeling studies (Fig. 3), we observed that it was possible to access the empty pocket of the northern region to gain potency by modification of the 7-position benzimidazole carboxamide. Designed compounds (**65** to **79** in Table 4) were synthesized according to Scheme 4. Chloro-dinitrobenzoic acid (**50**) was the general starting material for the final compounds (**65** to **75**). Methylation of **50** followed by SNAr displacement with primary amines provided **52**. The key transformation was the regioselective hydrogenation of **52** with 10% Pd/C to give **53** after column chromatography. After benzimidazole

formation the remaining nitro group of **54** was reduced to NH_2 by Zn powder in the presence of NH_4Cl to give **55**. A Sandmeyer reaction of **55**, followed by acid hydrolysis and amidation gave compounds **65** and **71**. Sulfones analogs (**73** to **75**) were synthesized by diazotization of **55**.

To synthesize sulfonamide analogs of this series at R^7 we started from 4-chloro-3-nitro-5-sulfamoylbenzoic acid (**62**), which was converted to **63** using a standard protocol (Scheme 4). A Mitsunobu reaction was employed for further substitutions of the sulfonamides followed by acid hydrolysis and amidation to achieve compounds **76** to **79**.

Compounds (**65** to **79**) were tested in the enzyme inhibition assay and the results are summarized in Table 4. Electron withdrawing groups at the R^7 position of **59** have significant effects on potency. Bulky R^7 groups of **59** may also provide rigidity and consequently limit the free rotation of R^1 substituents, as illustrated in Figure 5. The rigidity stabilizes the hydrogen bond network between R^1 hydroxyl group and the organized water, which also hydrogen-bonds to Glu276 and Glu288 side chains. The interactions of the primary amide of benzimidazole carboxamide with Glu201 and Lys202 were enhanced due to electron withdrawing groups at R^7 lowering electron density of the benzimidazole ring. The coordinates have been deposited in the Protein Data Bank[10] with code 3JZI.

Representative compounds in the optimized chemical series were tested for cell-based activity using a proprietary sensitive strain of *Escherichia coli* (*E. coli* HS294) in which the major drug efflux pumps have been deleted and cell permeability is enhanced by a reduction in LPS synthesis (Table 5). Improvement in cell-based activity were shown by these compounds relative to the initial hit **1** (MIC~25 μg/mL), in line with improvements in enzyme inhibition potency.

The antibacterial mechanism-of-action of these compounds was tested against *E. coli* HS294 strain specifically sensitized for AccC inhibitors. The targeted sensitization was achieved by lowering the pool of functional ACCase complex in the cell via overproduction of apo-BCCP. Overproduction of apo-BCCP downregulates transcription of the *accB*/*accC* operon and may also form an inactive complex between AccC protein and apo-BCCP.[12] Therefore, decrease in the MIC for the strain overproducing apo-BCCP (*E. coli* HS294/accB) relative to *E. coli* HS294 control strain indicates inhibition of AccC as the mode for antibacterial activity. As shown in Table 6, compounds (**40**), (**69**) and (**73**) gave a 4- to greater than 12-fold decrease in MIC upon overproduction of apo-BCCP, indicating on-target antibacterial activity while there is no change in the MIC for the antibiotic trimethoprim which does not inhibit ACCase. Furthermore, selective inhibition of fatty acid biosynthesis in *E. coli* HS294 by these

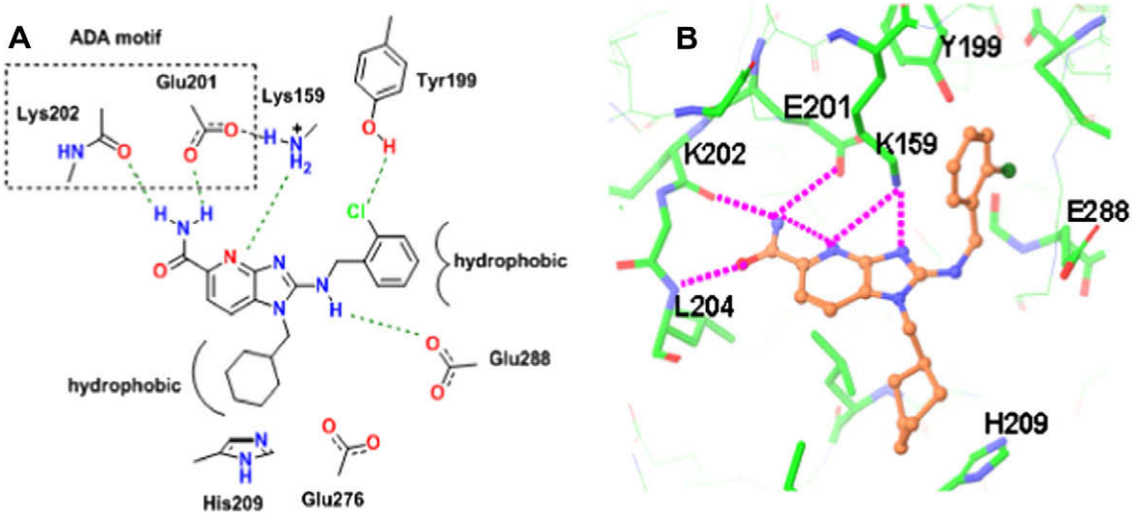

Figure 4. (A) Computer-aided modeling predicted possible binding interactions between *aza*-benzimidazole carboxamide and charged Lys159. (B) Structure of **36** bound to the AccC active site by molecular docking.

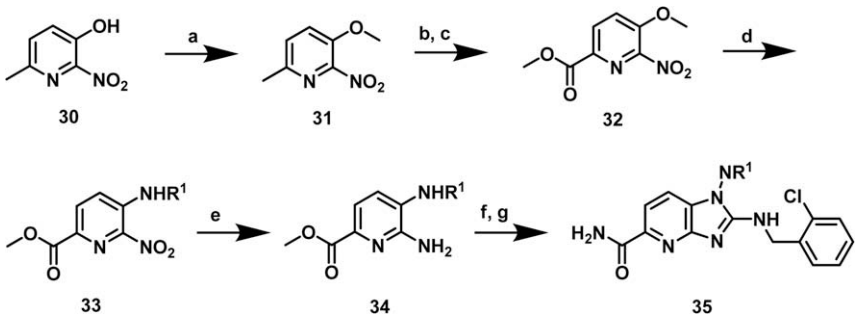

Scheme 3. Synthesis of compound **35**. Reagents and conditions: (a) TMS–CHN_2, MeOH; (b) SeO_2, dioxane, 90 °C overnight; (c) TMS–CHN_2, MeOH; (d) R^1NH_2, *i*-Pr_2NEt, *t*-BuOH, 160 °C, 15 min; (e) H_2/Pd-C, EtOAc; (f) DIC, 2-chlorobenzyl isothiocyanate; (g) NH_3, MeOH, 50 °C, overnight.

Table 3
Aza-benzimidazole carboxamide analogs

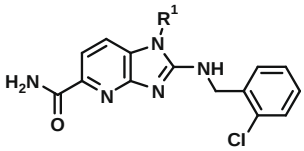

Compound	Structure of R^1	ACCase, IC_{50}[a,b] (μM)
36	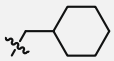	0.16
37		0.13
38	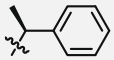	2.06
39	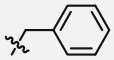	0.17
40	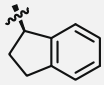	0.02
41	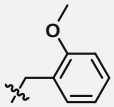	2.84
42	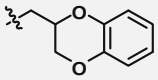	0.3
43	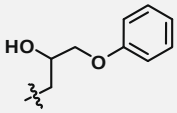	3.01
44	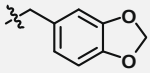	2.75
45	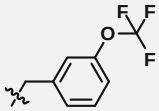	40
46	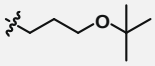	0.35
47		0.27
48	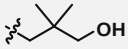	0.02
49	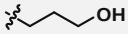	0.19

[a] Values are means of duplicate experiments on two separate weightings.
[b] [ATP] = 100 μM.

Table 4
In vitro data for compounds **65** to **79**

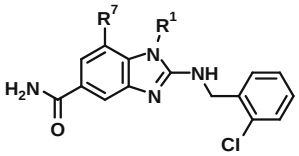

Compound	Structure of R^1	Structure of R^7	ACCase, IC_{50}[a,b] (μM)
65	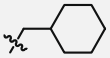		1.6
66	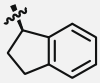		0.09
67			3.5
68			50
69	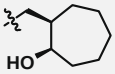		0.01
70	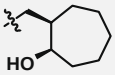		5
71	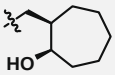		0.13
72	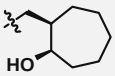		0.17
73	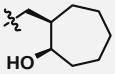		0.26
74	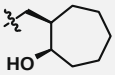		0.06
75	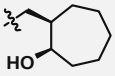		0.1
76	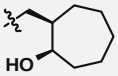		0.7
77	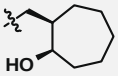		0.38
78	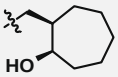	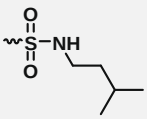	0.8
79	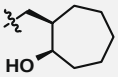	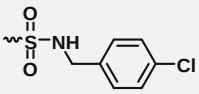	2.1

[a] Values are means of duplicate experiments on two separate weightings.
[b] [ATP] = 100 μM.

compounds supports inhibition of ACCase activity as the mechanism-of-action as shown for **69** in Table 7. The optimized compounds were also shown to have broad spectrum enzyme inhibition activity and are selective for bacterial AccC. No activity was found against eukaryotic carboxylases and human kinases (data not shown).

The AccC ATP-competitive inhibitors we report herein represent a class with a novel mode of action and broad spectrum enzyme inhibition activity. We utilized ALIS and mixture-based optimization during the early hit optimization stage to provide informative affinity SAR which translated well into the biochemical assay. Combining X-ray crystallography with computer-aided modeling achieved a ~360-fold improvement in enzyme inhibition and >100-fold improvement in cell-based activity (0.2 μg/mL MIC; HS294 *E. coli* strain). Additionally, the *aza*-benzimidazole carboxamide scaffold was discovered, providing a new chemotype for further discovery efforts.

Scheme 4. Synthesis of compound **65** to **79**. Reagents and conditions: (a) TMS–CHN_2, MeOH; (b) R^1NH_2, *i*-Pr_2NEt, DMF, 90 °C, overnight; (c) H_2, Pd/C; (d) DIC, 2-chlorobenzyl isothiocyanate; (e) Zn powder, NH_4Cl; (f) CuBr or CuCl, *t*-BuONO, CH_3CN; (g) HCl, H_2O–dioxane, 90 °C overnight; (h) $(NH_4)_2CO_3$, *i*-Pr_2NEt, EDC, HOBt, DMF; (i) $NaNO_2$, HCl, NaSR′; (j) oxone; (k) R^3R^4N, DEAD, PPh_3, MeOH.

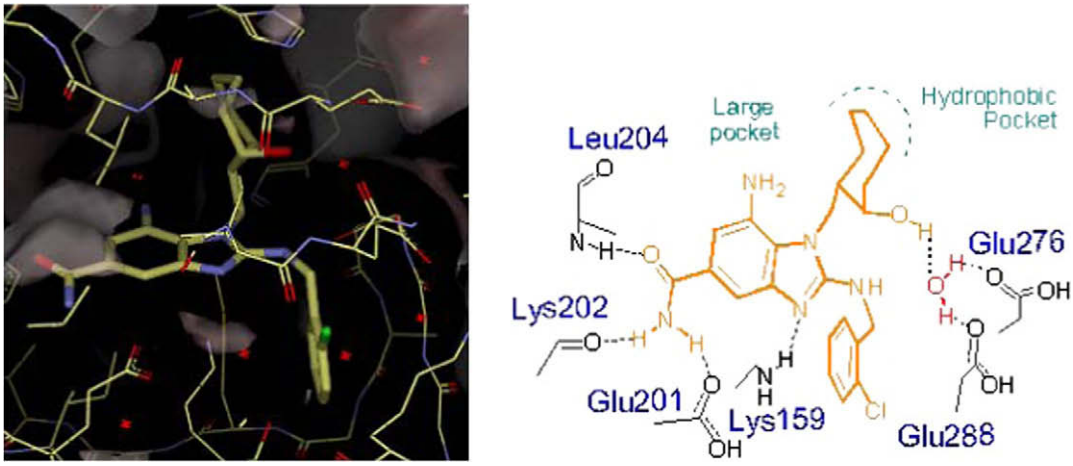

Figure 5. Depiction of the X-ray crystal structure of **70** bound to AccC. Water serves as an H-bond bridge between the inhibitor and two amino acid residues (Glu276, Glu288). PDB code 3JZI.

Table 5
Cell-based activity of compounds optimized for enzyme inhibition potency[11]

Compound	ACCase IC_{50} (μM)	*E. coli* HS294, MIC (μg/mL)
69	0.01	0.2
40	0.02	0.8
48	0.05	1.6
74	0.06	1.6
71	0.13	0.4
73	0.26	12.5

Table 6
Mechanism-of-action analysis using *E. coli* HS294 sensitized for AccC inhibitors[11]

Compound	ACCase IC_{50} (μM)	*E. coli* HS294, MIC (μg/mL)	*E. coli* HS294/accB (AccC sensitized strain), MIC (μg/mL)
69	0.01	0.8	<0.05
40	0.02	0.8	<0.05
73	0.26	12.5	3
Trimethoprim	Not active	0.1	0.1

Table 7
Pathway specificity of compound **69**

Target pathway[11]	*E. coli* HS294, IC_{50} (μg/mL)
Fatty acid Biosynthesis	0.5
DNA Biosynthesis	>20
RNA Biosynthesis	>20
Protein biosynthesis	>20

Acknowledgments

We thank Dr. Xianshu Yang for performing the initial ALIS screening and Mr. Michael Starks for analytical support. We also thank Dr. Paul McNicholas and Nathaniel Brown for supporting some of the pathway assays.

Supplementary data

Supplementary data associated with this article can be found, in the online version, at doi:10.1016/j.bmcl.2009.10.057.

References and notes

1. (a) Annis, D. A.; Athanasopoulos, J.; Curran, P. J.; Felsch, J. S.; Kalghatgi, K.; Lee, W. H.; Nash, H. M.; Orminati, J.-P.; Rosner, K. E.; Shipps, G. W., Jr. *Int. J. Mass Spectrom.* **2004**, *238*, 77; (b) Annis, D. A.; Nickbarg, E. B.; Yang, X.; Ziebell, M. R.; Whitehurst, C. E. *Curr. Opin. Chem. Biol.* **2007**, *11*, 518.
2. (a) Gould, I. M. *Int. J. Antimicrob. Agents* **2008**, *32S*, S2; (b) Chastre, J. *Clin. Microbiol. Infect.* **2008**, *14*, 3.
3. (a) Miller, J. R.; Dunham, S.; Mochalkin, I.; Banotai, C.; Bowman, M.; Buist, S.; Dunkle, B.; Hanna, D.; Harwood, J.; Huband, M. D.; Karnovsky, A.; Kuhn, M.; Limberakis, C.; Liu, J. Y.; Mehrens, S.; Mueller, W. T.; Narasimhan, L.; Ogden, A.; Ohren, J.; Vara Prasad, J. V. N.; Shelly, J. A.; Skerlos, L.; Sulavik, M.; Thomas, V. H.; VanderRoest, S.; Wang, L. A.; Wang, Z.; Whitton, A.; Zhu, T.; Stover, C. K. *Proc. Natl. Acad. Sci. U.S.A.* **2009**, *106*, 1737; (b) Mochalkin, I.; Miller, J. R.; Narasimhan, L.; Thanabal, V.; Erdman, P.; Cox, P. B.; Prasad, J. V. N. V.; Lightle, S.; Huband, M. D. *Chem. Biol.* **2009**, *4*, 473.
4. Harder, M. E.; Beacham, I. R.; Cronan, J. E., Jr.; Beacham, K.; Honegger, J. L.; Silbert, D. F. *Proc. Natl. Acad. Sci.* **1972**, *69*, 3105.
5. (a) Chapman-Smith, A.; Morris, T. W.; Wallace, J. C.; Cronan, J. E., Jr. *J. Biol. Chem.* **1999**, *274*, 1449; (b) Cronan, J. E., Jr. *J. Biol. Chem.* **2001**, *276*, 37355.
6. Cronan, J. E.; Waldorf, G. L. *Prog. Lipid Res.* **2002**, *41*, 407.
7. Freiberg, C.; Brunner, N. A.; Schiffer, G.; Lampe, T.; Pohlmann, J.; Brands, M.; Raabe, M.; Habich, D.; Ziegelbauer, K. *J. Biol. Chem.* **2004**, *279*, 26066.
8. Annis, D. A.; Shipps, G. W., Jr.; Deng, Y.; Popovici-Mueller, J.; Siddiqui, M. A.; Curran, P. J.; Gowen, M.; Windsor, W. T. *Anal. Chem.* **2007**, *79*, 4538.
9. (a) Huang, K.-T.; Sun, C.-M. *Bioorg. Med. Chem. Lett.* **2002**, *12*, 1001; (b) Lahue, B. R.; Ma, Y.; Shipps, G. W., Jr.; Seghezzi, W.; Herbst, R. *Bioorg. Med. Chem. Lett.* **2009**, *19*, 3405.
10. Berman, H. M.; Westbrook, J.; Feng, Z.; Gilliland, G.; Bhat, T. N.; Weissig, H.; Shindyalov, I. N.; Bourne, P. E. *Nucleic Acids Res.* **2000**, *28*, 235.
11. (a) Soriano, A.; Radice, A. D.; Herbitter, A. H.; Langsdorf, E. F.; Stafford, J. M.; Chan, S.; Wang, S.; Liu, Y.-H.; Black, T. A. *Anal. Biochem.* **2006**, *349*, 268; (b) Hecht, D. W. *Methods for Dilution Antimicrobial Susceptibility Tests for Bacteria That Grow Aerobically*, Approved Standard-Seventh Edition; Clinical and Laboratory Standard Institute, 2006.; (c) Enzyme and cell-based assay procedures are described in the Supplementary data.
12. James, E. S.; Cronan, J. E., Jr. *J. Biol. Chem.* **2004**, *279*, 2520.